



Article

Assessing the Cooling Benefits of Tree Shade by an Outdoor Urban Physical Scale Model at Tempe, AZ

Qunshan Zhao ^{1,*}, Jiachuan Yang ², Zhi-Hua Wang ² and Elizabeth A. Wentz ¹

¹ Spatial Analysis Research Center, School of Geographical Sciences and Urban Planning, Tempe, AZ 85287, USA; wentz@asu.edu

² School of Sustainable Engineering and the Built Environment, Tempe, AZ 85281, USA; jyang104@asu.edu (J.Y.); zhwang@asu.edu (Z.-H.W.)

* Correspondence: qszhao@asu.edu; Tel.: +1-480-280-6586

Received: 11 November 2017; Accepted: 5 January 2018; Published: 8 January 2018

Abstract: Urban green infrastructure, especially shade trees, offers benefits to the urban residential environment by mitigating direct incoming solar radiation on building facades, particularly in hot settings. Understanding the impact of different tree locations and arrangements around residential properties has the potential to maximize cooling and can ultimately guide urban planners, designers, and homeowners on how to create the most sustainable urban environment. This research measures the cooling effect of tree shade on building facades through an outdoor urban physical scale model. The physical scale model is a simulated neighborhood consisting of an array of concrete cubes to represent houses with identical artificial trees. We tested and compared 10 different tree densities, locations, and arrangement scenarios in the physical scale model. The experimental results show that a single tree located at the southeast of the building can provide up to 2.3 °C hourly cooling benefits to east facade of the building. A two-tree cluster arrangement provides more cooling benefits (up to 6.6 °C hourly cooling benefits to the central facade) when trees are located near the south and southeast sides of the building. The research results confirm the cooling benefits of tree shade and the importance of wisely designing tree locations and arrangements in the built environment.

Keywords: tree location; tree density; geometric arrangement; tree shade cooling benefits; outdoor physical scale model; microclimate field measurement

1. Introduction

The demands of a rapidly growing population has resulted in a shift toward larger and more expansive urban areas [1]. This has altered the surface energy and moisture balance of these urban areas and led to environmental issues such as the urban heat island (UHI) effect, human thermal discomfort, air quality degradation, and microclimate modification [2–7]. To alleviate urban thermal stress, to promote urban ecosystem services, and to improve human and environmental health, various heat mitigation and energy saving strategies are applied, including employing reflective/white roof, adding photovoltaics to capture the solar energy, and using vegetation to create urban green infrastructure. Among all of these strategies, vegetation as one of the most important components of urban green infrastructure, is becoming an integral feature of urban designs [8]. Commonly used urban green infrastructure includes residential landscaping, green corridors, green roofs and walls, and urban parks using a combination of trees, shrubbery, and turf grass [9–14]. The question that remains is how to best integrate urban green infrastructure with the transportation, residential, commercial, and industrial infrastructure to maximize the environmental benefits that are offered by the green infrastructure.

The research presented here focuses specifically on how to effectively and efficiently incorporate shade trees in residential neighborhoods in a hot desert city. In hot desert areas, trees provide multiple microclimate benefits by reducing solar radiation penetration, blocking the exchange of long-wave

(infrared) radiation inside urban canyons, and generating evapotranspiration [12]. In addition, trees provide ecosystem services, including air quality improvement, storm water attenuation, carbon sequestration, and a vast range of economic, social, and health benefits [9,15–17]. Use of tree shade requires a balanced and nuanced analysis of the tradeoffs between cooling by shade and the use of water, a scarce resource in semi-arid and arid regions [12,18]. Since the tradeoffs between water and energy require efficiency in the number of trees to be planted on a given parcel, effective tree placement strategies are needed (e.g., tree location, arrangement, and spacing) [19–22]. These strategies will help homeowners to maximize the overall benefits from trees with the fewest number of trees in an effort to simultaneously reduce both water consumption and energy use [23].

The effect of shade trees in urban areas has been examined through real world in situ measurements and through numerical modeling, both confirming the conventional wisdom that tree shade reduces surface and air temperature [24,25]. The in situ experiments apply meteorological instrumentation to measure environment accurately, but various real world conditions would influence the measurement results. The numerical modeling simulates physical environment through parameterization, but lacking of fieldwork validation makes the simulation results be less reliable. The differences among the in situ studies are the methods used, whether they measured surface or air temperature, and the impact of different types of shade, such as native, exotic, and artificial shade [26–28]. Results show reduced temperatures between 1 Celsius degree ($^{\circ}\text{C}$) and 9°C , depending on these variables. The problem with the results is that a variety of in situ conditions influences the results, such as the geometry and material characteristics of trees (tree type, tree height, leaf area, etc.), building arrangements, and background meteorological conditions. Numerical simulation models offers the ability to manipulate tree placement, background materials, and analyze cooling from tree shade by simulating the microclimate and resulting human thermal comfort [29,30]. Urban canopy models (UCMs) simulate tree foliage together with buildings to represent the emission and reflection of radiation, and mutual shading between buildings and trees, showing energy savings, and heat mitigation from shade trees. Computational fluid dynamics (CFD) modeling better represents the three-dimensional thermal environment than the UCMs and has been used to analyze air movement, pollution dispersal, and pedestrian wind tunnels [18,31,32]. Like UCMs, CFD simulations consistently show that increased vegetation provides cooling effects under a variety of conditions [10,33–35]. The challenge with modeling tree shade on buildings is that numerical simulations are unable to resolve the heat transfer of the wall (i.e., the buoyancy effect) [18].

In contrast to in situ measurements and numerical simulations, physical scale models combine the experimental control of numerical simulation with the real world complexities that are related to the natural environment [36]. There are comprehensive physical scale models that have been developed to measure urban albedo, aerodynamic drag, urban surface energy fluxes, thermal inertia, urban canopy microclimate, pedestrian energy exchange, convective heat transfer, thermal amelioration from water bodies, and evapotranspiration in urban canyons [37–48]. They offer the ability to control many of the field parameters, such as street layouts, existence of vegetation, solar radiation, wind speed, and humidity, which provides enough flexibility for analyzing radiation, shading, and wind tunnel conditions. With the exception of Roberts in Arizona, USA [36] and Pearlmutter et al. in Israel [45–48], none represent the hot desert urban environment, and very few incorporate vegetation [49,50]. This is because the morphology and materials of vegetation are much more complex than urban structures (such as cubes, blocks, or cylinders) in the physical scale modeling. Park et al. [51] included vegetation (Gold Crest Wilma plants) in the Comprehensive Outdoor Scale Model (COSMO) in Japan to evaluate the thermal comfort of pedestrians, finding that trees along pedestrian walkways can reduce the wind speed by up to 51% and decrease the temperature up to 2.2°C . Taleghani et al. [52] also created a scale model site with vegetation to analyze roof configurations in courtyards. Their scale model experimental results showed that a green pavement with grass on a roof or courtyard could result in up to 4.7°C air temperature cooling comparing to gravels and black materials.

Note that artificial trees were used in our outdoor scale model field measurement. As a result, the biophysical functions of real trees, e.g., transpiration by stomatal control, root uptake, foliage dynamics, and diurnal/seasonal variabilities, were not represented. However, artificial trees effectively capture the radiative shading mechanism of real trees. This is particularly true for xeric trees in an arid or semi-arid environment, such as Phoenix, where evapotranspiration is largely inhibited by excessive heat as well as relatively sparse foliage [53].

The goal of this research is to build an outdoor urban physical scale model to measure and understand the shading effect of different tree densities, locations, and arrangements in a typical residential area in a hot desert city. The physical scale model makes it possible to create and investigate a wide variety of tree locations and arrangements scenarios that is not practical to test in situ. We conducted our experiment in Tempe, Arizona, a municipality in the greater Phoenix metropolitan area in Arizona, USA. We designed this study based upon Park et al. [51] and Taleghani et al. [52] who demonstrated how vegetation can be an asset in physical scale models. Existing research has not yet explored the shading benefits of trees under different locations and arrangements in a physical scale model experiment. This is an obvious research gap in the outdoor urban physical scale modeling literature that we intend to fill and will be a crucial step in designing green infrastructure for the long-term sustainability of urban areas.

2. Experimental Details

2.1. Experimental Site and Period

In the experimental site, we developed an outdoor physical scale model with buildings and trees to represent a typical residential parcel with detached single-family house and surrounding buildings in the City of Tempe, Arizona (33.4° N, 111.9° W). Tempe is a municipality within the Phoenix metropolitan area in the Sonoran Desert of the U.S. Southwest (Figure 1). The population of Tempe in 2010 was more than 160,000 residents, with more than 40% of the population living in single-family detached dwellings [54]. The City of Tempe has a semi-arid climate that is situated in the Sonora desert. Most of the rain happened during monsoon season in July (23.9 mm) and August (21.8 mm), as well as from December (33.3 mm) through January (43.7 mm) at 2016. The annual rainfall at 2016 was 190.5 mm. June is the driest month with less than 2.5 mm mean annual precipitation. Average maximum air temperature ranges from 39.2 °C to 41.5 °C from June to August, and ranges from 20.3 °C to 22.0 °C from December to January at 2016. Average minimum air temperature peaks at 25.2 °C in July and can reach as low as 2.8 °C in January at 2016 [55]. Under this specific hot and dry summer climatic conditions, various heat mitigation strategies, such as adding vegetation coverage, creating green/cool roofs, and constructing cool pavement are essential for both reducing heat-related morbidity/mortality and energy consumption. To avoid the weather fluctuation in the summer monsoon season at August, the microclimate field measurements were conducted only at the selected steady hot and cloud free days in the period of 12–31 August at 2016. The weather conditions during experimental period are shown in Table 1, including maximum air temperature, minimum air temperature, average air temperature, precipitation, and cloudiness, which were retrieved from the nearby Phoenix Sky Harbor International Airport weather station record [56]. The total solar radiation data were not archived in the nearby airport weather station, so we acquired the solar radiation data from Remote Automated Weather Stations (RAWS) station in the vicinity at Casa Grande [57].

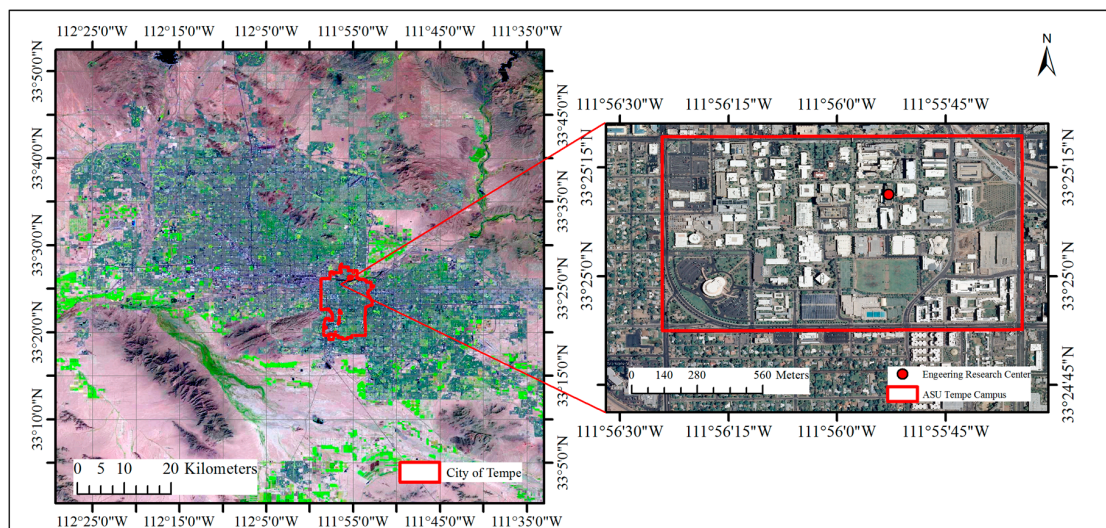


Figure 1. Study area.

Table 1. Weather conditions during the experimental period.

Date	Maximum Air Temperature (°C)	Minimum Air Temperature (°C)	Average Air Temperature (°C)	Precipitation (cm)	Total Solar Radiation (kWh/m ²)	Cloudiness
12 August 2016	40.6	27.8	34.7	0.00	7.28	Mostly clear
13 August 2016	42.2	28.9	35.7	0.00	7.29	Mostly clear
14 August 2016	41.1	30.0	35.3	0.00	7.39	Mostly clear
15 August 2016	43.3	30.0	36.7	0.00	7.30	Mostly clear
16 August 2016	43.9	30.6	37.0	0.00	7.20	Mostly clear
17 August 2016	42.8	28.9	36.7	0.25	7.12	Mostly clear
18 August 2016	40.0	27.8	34.5	0.03	5.73	Mostly clear
20 August 2016	37.8	26.7	31.9	0.00	6.67	Clear
30 August 2016	41.6	28.9	35.1	0.00	6.62	Clear
31 August 2016	41.1	27.8	34.9	0.00	6.72	Clear

The specific residential parcel that we analyzed is a generic one in the Tempe residential neighborhood with north-south building orientation. Within the neighborhood, most of the single-family houses were built with concrete block construction during the 1950s to 1960s. The average parcel size is around 700 m² with front/back yards, and the average single story building size is 134 m², according to the Maricopa County Assessor's records [58]. Most of the households have nearby neighbors on the west/east side, except those buildings that are close to the major north-south direction roads. This unique compact urban layout and building orientation make it difficult to plant any residential tree in the west or east side of the buildings. Even though there is not a strict regulation for front yard landscaping, most of the household owners plant shade trees to provide some level of shade to their own home structures.

The outdoor physical scale model is located at the rooftop of the six-story Engineering Research Center (ERC) building at Arizona State University Tempe campus, which is approximately 10 km southeast of Phoenix Sky Harbor International Airport and 2 km east of residential parcel we analyzed (Figure 1). This experimental site has many logistical advantages, such as high level of security and its central location on ASU Tempe campus. To be the highest structure in the area, the rooftop of the ERC building is free of obstructions (e.g., other buildings, trees) that can potentially result in unwanted microclimate influences such as horizontal shading, wind environment alternation or anthropogenic cooling or heating. The ERC rooftop surface is comprised of a layer of steel grating (6 cm × 3 cm gaps) on 2 m high support piers. The overall rooftop dimensions are 85 m × 23 m and the building's long axis is oriented in the south-north direction. To avoid the excess wind influences on the experimental

results and ensure the safety of the equipment and people, ERC rooftop has an approximately 1 m high surrounding protected walls. The south portion of the ERC roof is largely free of structures and is the optimal area to construct the scale model experiment.

The outdoor physical scale model was constructed with an array of concrete blocks to represent the residential buildings (Figure 2). Since the rooftop surface is a layer of steel grating, we used 260 concrete blocks to create a 20 blocks (386.0 cm) \times 13 blocks (250.9 cm) underlying concrete surface to represent the impervious surface of the residential area. Each concrete block is a cube with equal length, width, and height of 19.3 cm. The cubes are hollow concrete with a 2 cm-thick wall and are painted dark gray. Further, because the cubes are relatively small in size, 18 of them were aggregated as a single family building with six blocks (115.8 cm) as the building length and three blocks (57.9 cm) as the building width. The concrete block of rooftop is 38.6 cm long, 19.3 cm wide, and 4.2 cm high with dark grey painted as well. The buildings in the scale model were designed to be scaled at about 1:15.5 relative to a general 18 m length, 9 m width, and 3.65 m height flat roof residential house in Tempe residential neighborhood. To avoid the boundary effect and to explore the tree shade effect on the surrounding buildings, we created two 3 blocks \times 2 blocks small buildings with rooftops to the west and east side of the experimental building. Three sets of the building arrays were created with four blocks (77.2 cm, 12 m in the real world) distance in the south-north direction to generate two similar urban canyons to serve as the treatment group and control group separately. The depth of the canyons was 23.5 cm and the street aspect H/W (the ratio of the canyon height H to the street width W) was 0.3. We maintained a 19.3 cm distance between the building and the centroid of the tree.

Natural two-tone pine median profile artificial trees that made by polyvinyl chloride (PVC) with 45.7 cm tall and 27.9 cm base diameter (at the widest point) were used in the scale model site to represent 7.1 m thornless mature mesquite trees (*Prosopis thornless* hybrid 'AZT™') in the residential neighborhood. There are several important reasons that we select an artificial tree in this scale model experiment. First, radiation exchange is often the dominant factor to influence the microclimate conditions in the hot dry desert environment [59]. In this scale model experiment, we want to isolate the role of shading from trees to buildings rather than considering every aspect of the vegetation to better understand the tree shade coverage benefits to the building facade. Second, when compared to real trees, we can easily find identical artificial trees with the same albedo, emissivity, and physical structures at an affordable price. This will guarantee the similarity of shading area, shape, and density. Many errors or uncertainty may exist and influence the experimental results by using the real trees, such as the different soil moisture level, leaf area humidity, plant evapotranspiration rate, plant albedo and emissivity, and shadow shape, area, and density that were mentioned in Park et al. [51]. Third, although existing research has utilized both real and artificial grass in the scale model experiment [52,60,61], none of the research attempts to use artificial trees in the outdoor scale model experiment. This experiment will help to understand the importance of shading and retaining heat radiation from artificial trees in the hot dry desert environment.

In the scale model experiment, the scale model always has different thermal inertia (volumetric heat capacity) as compared to those of real buildings. This is the common problem of scale modeling and is difficult to compensate. A method to avoid this problem is to create a larger urban mock neighborhood and to make it more similar (thermally and dynamically) to the real world situation. Nevertheless, it will lose some flexibility of physical scale modeling and increase modeling cost. Due to the space and cost limitation, our experiment kept the scale model in a relatively small size to maintain more flexibility of the physical scale modeling. Further, we used the hollow concrete cubes to represent the concrete block construction of single-family houses in the study area to represent the thermal mass of the building structures. The reason we chose to use concrete blocks in the experiment to represent buildings was because most of the single-family houses built before 1980s were concrete block construction.

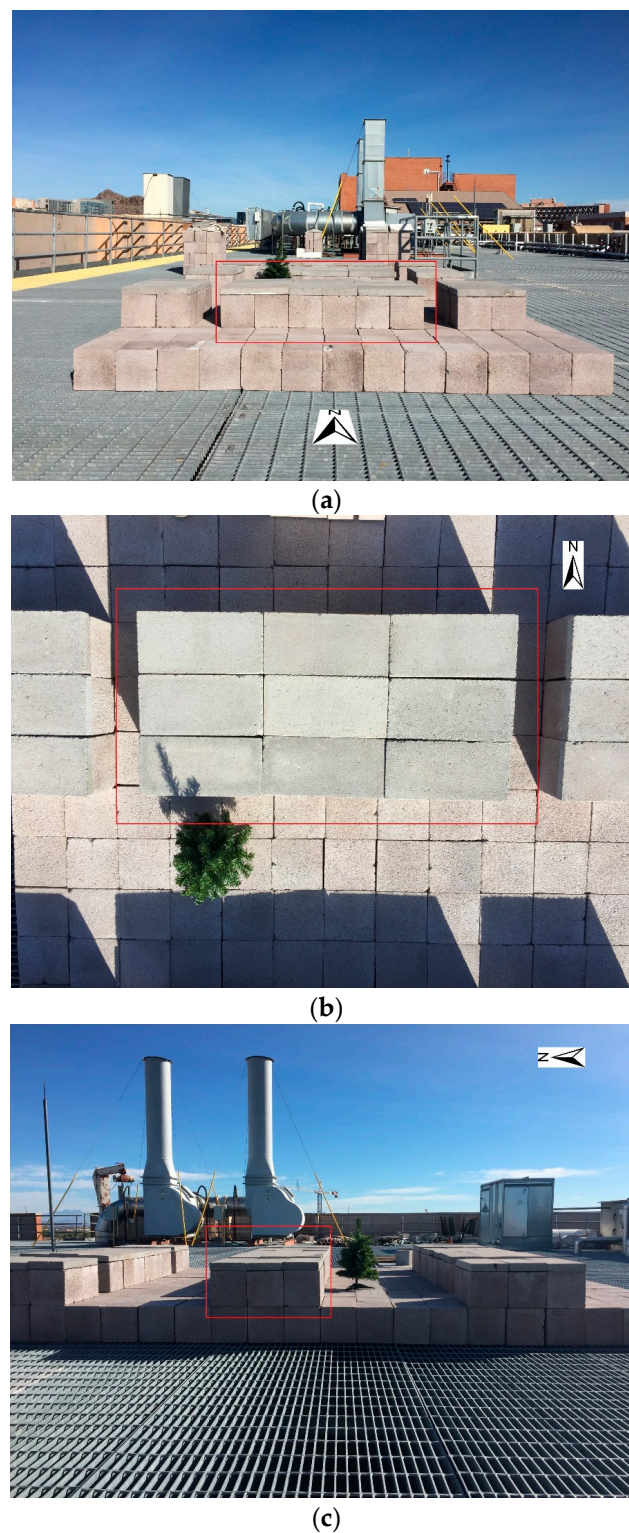


Figure 2. Pictures of the outdoor urban physical scale model (Red outline represents a single unit of the target building). (a) Front view; (b) Plan view (for one urban canyon); and (c) Side view.

2.2. Experimental Design

In this physical scale model experiment, three determinants of tree shading effect were tested: tree density, tree locations, and tree arrangements. Tree density is the total number of trees used per experiment. Tree location is the placement of the trees relative to the building structure. Tree

arrangement is analyzed with two or more trees and characterizes whether they are arranged closely (clustered) or separately (dispersed). For tree density, we analyzed between 0 and 2 trees to simulate the prevalent choices. The reason we only consider up to two trees for the single building is because landscape regulation and water usage limitation in the desert environment make it inefficient to plant three or more number of tall trees (7 m) in a residential household front yard. Seven potential tree locations in the building south front yard were studied with a 19.3 cm distance from the structure (3 m in the real world) (Figure 3). To characterize different tree density, location, and arrangement, we conducted 10 different experiments (details summarized in Table 2). Group 1 is the empty control group without trees to represent the natural solar radiation and reflection in the urban canyon. Group 2 contains one tree with seven different tree locations. Group 3 includes the cluster arrangement of two similar trees with different locations. Group 4 represents the disperse arrangement of two trees. Given the size of the artificial trees, we placed two trees at location 3 and 5, rather than location 3 and 4 to represent the cluster tree arrangement. Table 3 shows the key factors in the different experimental groups. Since the weather conditions fluctuate frequently in the summer monsoon season, it is difficult to conduct multiple observations for each scenario. Thus, we tested each tree location/arrangement scenario in the similar weather conditions (Table 1) without multiple observations. Seven one-tree scenarios were tested over a consecutive seven-day period from 12–18 August 2016, and three two-tree scenarios were tested on separated days at 20 August, 30 August, and 31 August.

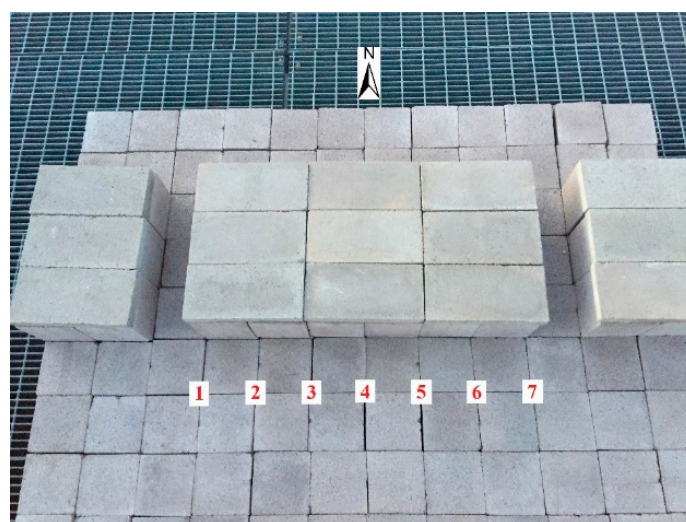


Figure 3. Potential tree locations in the outdoor urban physical scale model.

Table 2. Summary of tree number, location, and arrangement in different experimental groups.

Group No.	Tree Numbers	Tree Locations	Tree Arrangements
Group 1	0	N/A	N/A
Group 2	1	(1), (2), (3), (4), (5), (6), (7)	N/A
Group 3	2	(3,5), (4,6)	Cluster
Group 4	2	(2,5)	Disperse

Table 3. Key factors in different experimental groups.

Treatment Group	Control Group	Key Factors
Group 2	Group 1	Tree density and location (one tree vs. no tree)
Groups 3 and 4	Group 1	Tree density (two trees vs. no tree)
Groups 3 and 4	Group 2	Tree density (two trees vs. one tree)
Group 4	Group 3	Tree arrangement (cluster vs. disperse)

2.3. Measurement Equipment

To measure the microclimate conditions, 12 DS1921G iButton temperature loggers [62] were attached with strong adhesive to the scale model building facade to measure the near-surface building facade temperature. Since the direct solar radiation influences the temperature measurements recorded by the iButton temperature logger, we covered each iButton logger with white printer paper. The iButton loggers were individually calibrated in a NIST-traceable chamber by the manufacture, measuring temperatures in 0.5 °C increments at an accuracy of ± 1 °C, over a range of -30 °C to $+70$ °C.

Because the outdoor urban physical scale model represents a compact urban setting in the real residential neighborhood, there is no adequate space for planting a tree in the west and east side of building. Thus, the physical model represents a west-east orientated street canyon, and the 12 iButton loggers were installed on the south facades of the target and surrounding buildings (Figure 4). Loggers 1–8 were installed in the south urban canyon, and loggers 9–12 were installed in the north urban canyon. In the south urban canyon, loggers 2–7 measured the facade temperature of the target building, and logger 1 and 8 measured the facade temperature of the surrounding buildings. In the north urban canyon, logger 9 served as the control group of logger 1, loggers 10 and 11 served as the control group of loggers 2–7, and logger 12 served as the control group of logger 8. In our experiment, all of the temperature loggers were set to collect the temperature data at 15-min intervals over a period of 24 h.



Figure 4. The digital photo of iButton logger locations.

To validate the iButton measurements and to collect information on the overall thermal environment, we used a FLIR P620 thermal camera [63]. The resolution of FLIR P620 thermal camera is 640×480 with the temperature measurement accuracy at ± 2 °C or 2% of reading. It has a large temperature measurement range (-40 °C– 500 °C) and a high thermal sensitivity (<0.06 °C at 30 °C). FLIR thermal camera was applied to collect the surface temperature in our experimental site, which was later compared with the iButton temperature measurement. The experiments were conducted on clear sky days with stable solar radiation. Wind speed was not measured in this physical scale model experiment. First, wind speed is relatively low in this outdoor urban physical scale model because of the 1 m protecting walls around the rooftop (Figure 2a,c). Second, the wind speed is similar in both the urban canyons because of the size of our physical scale model.

3. Experimental Results

3.1. Instrumentation Calibration and Quality Control

A preliminary experiment was conducted on a clear hot summer day from 10:30 to 17:30 at 13 July to validate the temperature measurement accuracy by comparing temperature readings from thermal images and iButton temperature loggers. We calibrated the thermal imagery by using FLIR

Tools version 5.9 to adjust temperature related parameters, such as emissivity, reflected apparent temperature, distance, atmospheric temperature, and relative humidity. Because the scale model is mainly constructed by grey concrete blocks, we set the emissivity as 0.91 [18,64]. Atmospheric temperature and relative humidity were decided by the nearby weather station at Sky Harbor International Airport [65]. We took two thermal images every 30 min from the west side (2 m distance) and east side (1.5 m distance) of the scale model. Because there was not an obvious heat source on the rooftop, we set the reflected apparent temperature the same as the atmospheric temperature.

To validate the accuracy of measuring block surface temperature by iButton loggers, we chose two iButton loggers in the middle of two urban canyons to do the comparison between the thermal images and iButton loggers (Figure 5a). We extracted 15 temperature readings from 10:30 to 17:30 at each iButton logger, and identified surface temperatures in 60 thermal images (30 images for each canyon, 15 images taken from west and 15 images taken from east), which were next to the iButton loggers (Figure 5b). As shown in Table 4, the root mean squared error (RMSE) between iButtons and thermal images was 1.7 °C in the north urban canyon with tree shade, and was 2.0 °C in the south urban canyon without tree shade. The mean absolute error (MAE) was 1.5 °C in the north urban canyon and 1.9 °C in the south urban canyon. An existence of tree induced a 0.3 °C difference of RMSE and a 0.4 °C difference of MAE. iButton temperature was consistently lower than the concrete block surface temperature derived by thermal images (Figure 6).

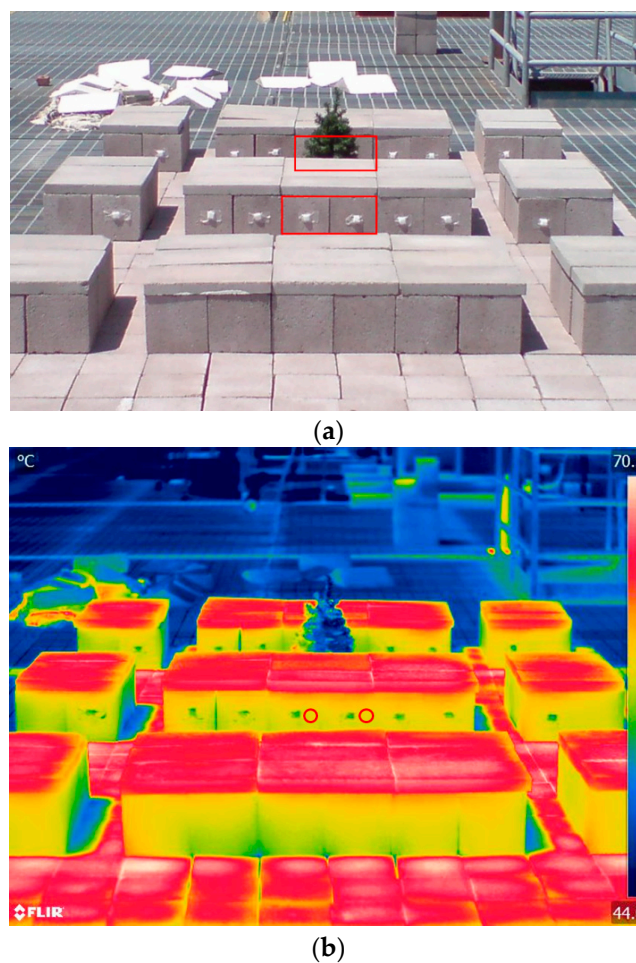
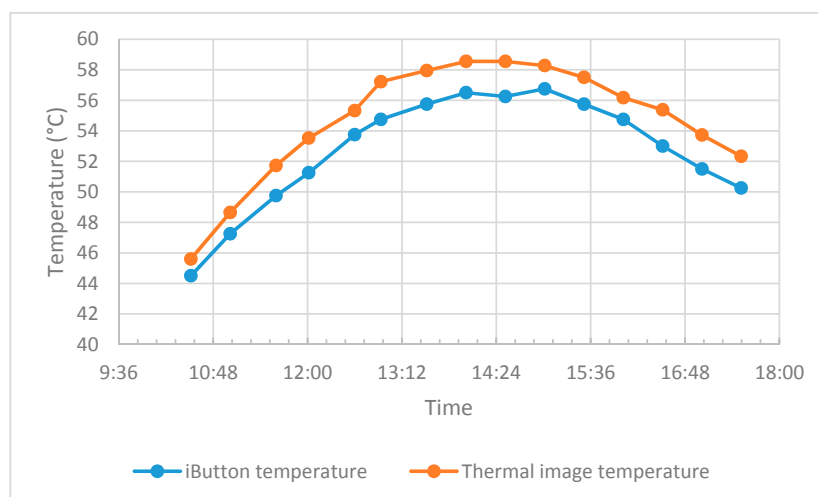


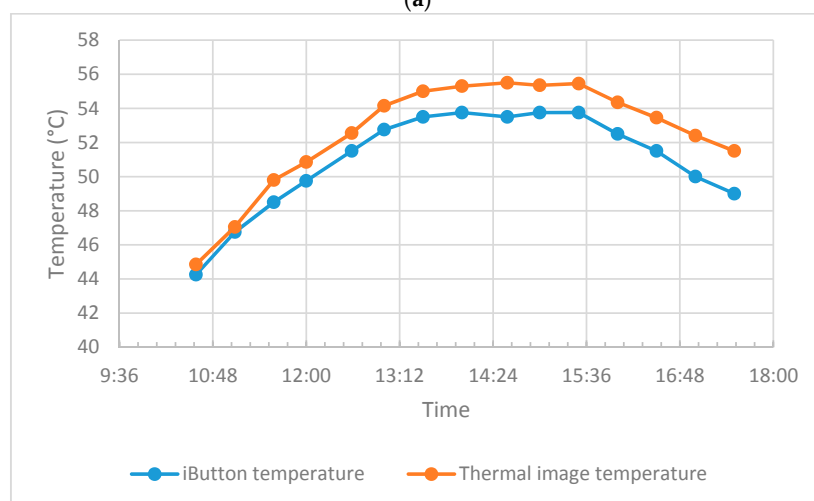
Figure 5. Thermal image and digital photo from FLIR P620 thermal camera (Taken at 13:59, 13 July). (a) Digital photo (red outline indicates iButtons that were used in the validation); (b) Thermal imagery (we extracted the surface temperatures from red circles for validation).

Table 4. Temperature measurement errors (root mean squared error (RMSE) and mean absolute error (MAE)) between the thermal images and iButton loggers.

	RMSE (°C)	MAE (°C)
North urban canyon (with tree)	1.7	1.5
South urban canyon (without tree)	2.0	1.9



(a)



(b)

Figure 6. Temperature comparison between iButtons and thermal images of proximal exposed concrete block surfaces. (a) South urban canyon (without tree); (b) North urban canyon (with tree).

Since the iButton was wrapped by white printer paper and the paper had higher reflective rate comparing to the grey concrete block surface, less direct solar radiation was received by the iButton loggers. On the other hand, the concrete blocks had higher heat capacity, and easily heated up under direct solar radiation. It was not surprising that the temperature of the calibrated iButton loggers were lower than the real concrete block surface temperature. The average systematic error (temperature differences between iButtons and thermal images) was 1.9 °C in the south urban canyon and 1.5 °C in the north urban canyon. After accounting for the temperature bias between iButton and thermal camera measurements, the measurement errors of the cooling benefits of tree shade were around 0.3 °C between two canyons, according to the RMSE. When considering the accuracy of iButton (± 1 °C) and FLIR thermal camera (± 2 °C or 2% of reading), the preliminary experimental results showed that

iButton can be used to measure and compare the building facade surface temperature in this scale model experiment. The method used in measuring the skin temperatures was a compromise due to the practical difficulty and complexity in measuring surface temperatures using direct contact sensors such as flat surface thermistors or thermocouples.

3.2. Tree Shade Cooling Benefits to the Target Building

For the one-tree scenarios, we moved the single artificial tree from the west side of the front yard to the east side of the front yard during the experimental period to explore the cooling benefits of the tree shade to the buildings. Because our primary interest is focused on the cooling benefits of tree shade during the greatest insolation hours, we narrowed the time interval to 9:30 to 15:30 and extracted the temperature records in the iButton logger to obtain the temperature variation.

To understand how tree shade influences the building facade temperature, we calculated the temperature difference (ΔT_s) between the south urban canyon (T_{exp} , experimental group) and the north urban canyon (T_{ctl} , control group) through Equation (1):

$$\Delta T_s = T_{exp} - T_{ctl} \quad (1)$$

In the north urban canyon, the average temperature of loggers in the target building (logger 10 and 11) served as the control group to compare with temperature in the south urban canyon (loggers 2 through 7). We used the average temperature of logger 2 and 3 to represent west facade temperature, logger 4 and 5 to show central facade temperature, and logger 6 and 7 to represent east facade temperature. Since the size of the experimental site was relatively small, the angle of incident for both of the canyons was similar, and we did not consider this factor in this research.

Figure 7 shows the tree shade cooling effect on the target building in one-tree scenarios. Because of the sun movement during the diurnal cycle, the coverage of tree shade moves from the west side of the south facade to the east side of the south facade. Among all of the one-tree scenarios, we chose the scenario that the single tree located at the central part of the front yard (location 3 in Figure 3) to represent how the movement of tree shade coverage influenced the building facade temperature. In this scenario, morning shading in the west side of facade cooled down the west facade at the maximum value of 1.25 °C from 9:30 to 12:00. In the afternoon, tree shade covered the east side of the building facade, and we can distinguish a 1.5 °C temperature decrease at the east facade from 14:15 to 15:30.

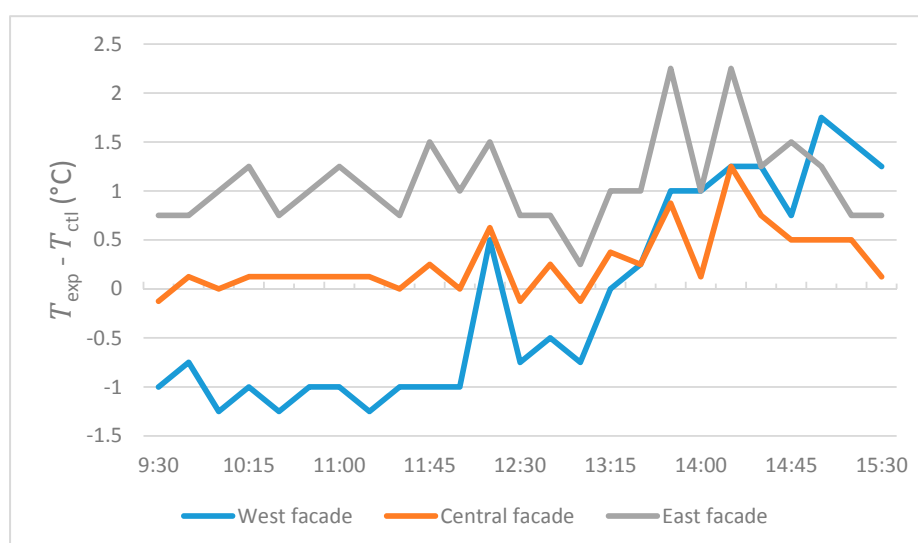


Figure 7. Cooling effect of tree shade on the target building facade temperature (One-tree, at the central part of front yard).

Figure 8 shows the cooling benefits of tree shade under different tree arrangements in two-tree scenarios. In the experimental groups, two cluster tree arrangements (location 3 and 5 or location 4 and 6) and one disperse tree arrangement (location 2 and 5) were tested. We compared the tree shade cooling benefits by one cluster tree arrangement (location 3 and 5, Figure 8a) and one disperse tree arrangement (location 2 and 5, Figure 8b). In the cluster tree arrangement, the west facade was heavily shaded from 9:30 to 11:15. The largest shading benefit was 2.5 °C at 10:30 in the central facade. The shading benefits in the afternoon were not as evident as the shading in the morning, but the results showed an opposite temperature trend at the central and east facade when comparing to west facade. With a disperse tree arrangement, steady shading benefits were shown for the west facade. Morning shading benefits were found at the central facade and afternoon shading benefits were identified at the east facade. The maximum morning shading benefit was 2 °C in the west facade at 11:15 and 11:45. In the afternoon, 1.25 °C shading benefit was shown in east facade at 15:30.

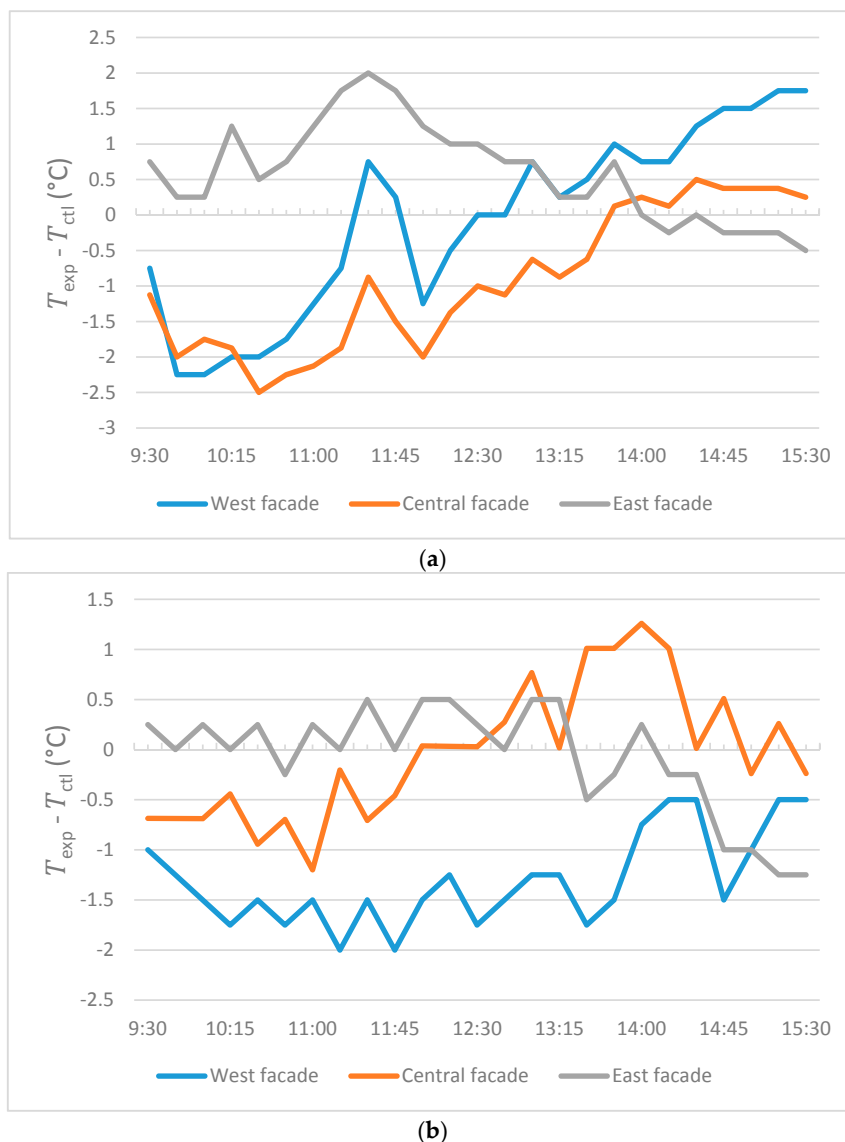


Figure 8. Cooling effect of tree shade on the target building facade temperature (Two-trees). (a) Cluster tree arrangement; and, (b) Disperse tree arrangement.

To compare the tree shade cooling benefits at different tree locations and arrangements, we calculated the hourly mean temperature differences between two urban canyons (ΔT_s) to represent

the average shading benefits from 9:30 to 15:30 (Table 5). In one-tree scenarios, the best tree location preferred central and east side of the front yard (location 4, 5, and 6). We observed more than 1 °C shading benefits at either central or east facade. Few shading benefits were found at the edge of front yard (location 1 and 7) because half of the shading was projected to the nearby buildings. In two-tree scenarios, the best tree arrangement preferred cluster arrangement at the east side of the front yard (location 4 and 6). In this tree arrangement, two trees can provide up to 6.6 °C hourly mean shading benefits to the central facade of the building. When planting trees in a cluster arrangement, the results showed that planting trees in the east side of the front yard (location 4 and 6) generated more shading benefits than locating trees in the central area (location 3 and 5). When locating trees at the southeast of the properties, we observed an extra 3 °C hourly cooling benefit in the west facade, 2.7 °C extra hourly cooling benefit in the central facade, and 7.6 °C extra hourly cooling benefit in the east facade. Further, a disperse tree arrangement (location 2 and 5) had a better shading effect at both the west facade (5.2 °C extra hourly cooling benefit) and east facade (2.8 °C extra hourly cooling benefit) of the building comparing to the cluster tree arrangement in the central part of the front yard (location 3 and 5). However, the shading effect from the disperse tree arrangement was worse than the cluster tree arrangements in the central facade because of the space between two trees. The enormous shading benefit when clustering trees at the east side of front yard (location 4 and 6) is unforeseeable, but it is consistent with the shading benefits that we find when locating a single tree at location 4 and location 6.

Table 5. Hourly shading benefits comparison for each experimental group (Referring to Figure 3 for tree locations, temperature unit is °C).

		West Facade	Central Facade	East Facade
One tree scenarios				
West to East	L1 ¹	1.5	3.6	5.9
	L2	0.4	3.8	7.1
	L3	−0.5	1.1	4.5
	L4	3.1	−1.6	5.1
	L5	2.6	−1.3	1.5
	L6	1.5	0.7	−2.3
	L7	3.4	2.5	−0.4
Two trees scenarios				
Cluster	L3 & L5	−0.3	−3.9	2.5
Cluster	L4 & L6	−3.3	−6.6	−5.1
Disperse	L2 & L5	−5.5	−0.2	−0.3

¹ L1 represents location 1 in Figure 3.

3.3. Tree Shade Cooling Benefits to the Surrounding Buildings

Besides the target building, it is also important to explore the cooling effect from tree shade on the surrounding buildings. When placing the single tree near the boundary of the building front yard, part of the tree shade was projected to the surrounding buildings. In this experiment, tree shade cooling benefits were compared by iButtons on the west/east surrounding building (logger 1 and 8) and on the outer-west or outer-east facade (logger 2 and logger 7) in the target building. Because only the early morning and late afternoon shading influenced the surrounding buildings, we extracted temperature records from 8:00 to 12:00 to understand the shading benefits of the west surrounding building, and temperature records from 12:00 to 17:00 to understand the east surrounding building. Figure 9 shows the tree shade cooling benefits on the target building and the surrounding building. It is clear from Figure 9 that the shading benefits are more evident when locating the single tree at the edge of the front yard (locations 1 and 7). The cooling benefits of tree shade on the west surrounding building is at the maximum value of 2 °C when locating single tree at the west edge of front yard

(location 1). Not surprisingly, the shading period and intensity all decreased when moving this single tree towards the east side of the building (cooling from 8:00 to 10:45 at the maximum value of 1.5 °C). Similarly, the shading benefits to the east surrounding building happens from 13:15 to 17:00 at the maximum value of 2.5 °C when locating the single tree at the east edge of the front yard (location 7). The shading intensity and period drops down when moving this tree west (cooling from 15:45 to 17:00 at the maximum value of 1.5 °C). When placing trees at the boundary of the building parcel (location 1 or 7), longer and stronger shading benefits are detected.

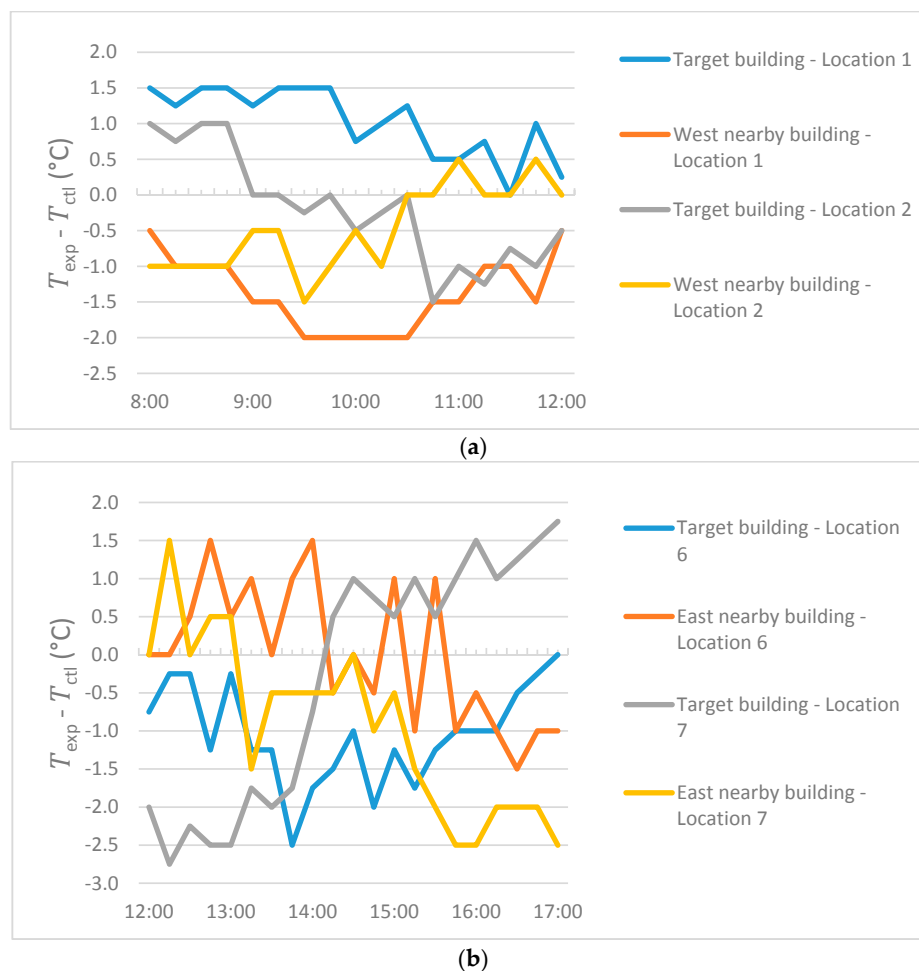


Figure 9. Cooling effect of tree shade on the surrounding building facade temperature (One-tree). (a) Morning shading to the west nearby building; (b) Afternoon shading to the east nearby building.

4. Discussion

Our experimental results demonstrate that tree density and arrangements influence hourly facade cooling benefits on the order of 0.5–6.6 °C, which is consistent with existing research [66]. The first contribution of this research is to provide a quantitative measurement of how tree density influences the facade cooling benefits. A single shade tree can induce a maximum hourly cooling of 2.3 °C of the facade temperature, and two trees can decrease the hourly facade temperature by up to 6.6 °C in the scale model experiment (Table 5). These findings confirm that a higher tree density can substantially enhance the shading benefits on the building facade. Second, the physical scale model provides the capability to examine various tree locations and arrangements scenarios that are not practical to test in situ. When locating one or two trees in the mock urban canyon, the field experimental results consistently show that tree shade cooling benefits are greater when locating trees at the central and east

side of the building south front yard (Table 5). Although conventional wisdom suggests that residents plant their shade trees at the southwest corner of their house, the research results demonstrate the effectiveness of planting trees in the southeast of the building structures when considering facade cooling. When the central area of the south front yard space is limited or occupied (etc. driveway), we suggest home owners to plant a new shade tree at the southeast corner of the residential properties to provide extra shading and cooling benefits to the building facade. Planting trees in the southeast will offer ample shade in the morning for the west facade, and provide substantial cooling benefits to the east side of building facade in the afternoon. It will be valuable to examine the effectiveness of locating trees at the southeast corner of the properties in the future research.

By comparing the shading benefits from the cluster and disperse arrangement, the results show that a disperse arrangement is not necessarily worse than the cluster arrangement. A cluster arrangement with better afternoon shading provides the most cooling benefits in this particular urban layout, but the disperse arrangement also offers a good level of cooling benefits to the whole building facade. All of the results confirm the importance of the benefits from tree shade coverage in relation to the residential buildings. In this compact urban setting, nearby surrounding buildings also receive evident tree shade cooling benefits (around 2 °C, Figure 9), especially when planting trees at the edge of the residential parcels.

From Figures 6–8, the temperature of exposed facade increases in the afternoon. The potential explanation is that artificial tree serves as a heat source in the afternoon and radiates heat to the nearby building facade. Although artificial tree provides various benefits and convenience in the experiment (Section 2.1), this is an unavoidable issue due to lack of evapotranspiration in artificial trees. This phenomenon diminishes and underestimates the cooling benefits of tree shade in the scale model experiment. However, this is further validated the importance of tree shade coverage for the building facade. When comparing to artificial turf with similar materials to the artificial tree, the existing research show that artificial turf increases the surface temperature and raises health issues on the sports playground [67–70]. However, the shading from artificial tree is still found to be valuable and reduces the facade temperature. The finding here emphasizes the contribution of shading to the facade surface temperature and corresponds with the finding in the existing literature that natural shading and artificial shading provide similar thermal comfort in the hot dry desert climates [24,28].

Several limitations exist in this scale model experiment. First, we used iButton loggers to measure the near surface air temperature and approximately represented the building surface temperature with the validation of thermal images. Even though some existing research used iButton loggers to measure surface temperature [71–74], flat surface thermistors or thermocouples may provide better surface temperature measurements with more experimental efforts. Second, this research did not account for the building's open structures, such as windows, doors, and ventilation. Adding these important building components into the physical scale mode is expected to improve the accuracy of the quantitative study. Further, we used concrete blocks to represent the building structure in the physical scale model experiment. Some houses may not be constructed by concrete structure, but with wood or stucco structures, and would have different physical properties (albedo, emissivity, etc.). Future study can be conducted to include this aspect of building properties. Last, this research particularly focuses on a hot arid urban environment that radiative shading from trees is the predominant factor to cool the outdoor environment. The best tree locations and arrangements results might vary under different geographical locations and climate conditions [75]. Other factors, such as evapotranspiration and wind speed, need to be considered.

This research represents a case study that attempt to assess the shading benefits under different tree locations and arrangements in a residential neighborhood by an outdoor urban physical scale model. A number of improvements can be made to improve this work in subsequent studies. For example, different tree species, alternative leaf area index/canopy density, crown size, and tree heights are all important options for flora [76,77]. All of these factors can be added and evaluated in the physical scale model. The comparison between artificial tree and real tree will

also be important to understand how evapotranspiration and retention heat issue influence surface temperature in the built environment. In addition, the specific compact urban arrangement that we simulate limits the orientation of buildings and location of trees in the experiment [78]. Different building arrangements and orientations can be adopted to this outdoor urban physical scale model in future studies. Furthermore, trees cool down the building structures in the daytime, but they also trap the long wave radiation during the night because of the low sky view factor under tree canopy [79]. This outdoor urban physical scale model can be used to explore the overall advantages and disadvantages of trees for mitigating UHI effects in both daytime and nighttime and serve as a field experiment site for the validation of numerical modeling of urban areas. The research results in the scale model experiment can also be used as an input scenario in a larger area numerical simulation modeling to explore how tree arrangement influences the neighborhood climate environment.

The research finding from this scale model experiment can translate into important landscape architecture design implication and policy recommendation to the compact residential neighborhood in the desert city. Because of the space limitation in the compact residential areas, green infrastructure in these areas is normally not adequate [80]. Thus, the policy encouragement of expanding urban green infrastructure from the city government and/or the homeowner association is important and necessary. According to our research findings, city residents or single-family homeowners should plant their first tree to shade the east side of the south facade, and allow enough space between multiple trees to maximize the overall shading benefits. In addition, trees located at the edge of residential parcel will be valuable through neighboring shading. They will provide ample shading to multiple houses and improve the overall living environment in the neighborhood. In Wentz et al.'s recent research [19], they mentioned that the homeowner association only provided a minimum landscaping guideline in Goodyear, AZ. Our research results will be useful to providing landscaping suggestions in the homeowner association guidelines for arranging trees wisely in the residential neighborhood. Although this research focuses on the tree shade benefits at building and neighborhood scales in the compact desert residential settings, the research contribution will be beneficial for understanding the landscaping deployment of urban green infrastructure, such as urban parks and street trees in the entire urban area [81–84]. We anticipate to raise the policy attention from city mayors, policy makers, and homeowner association to understand the importance of urban green infrastructure, emphasize the use of urban green infrastructure in the future city developmental plan [85], and wisely design tree locations and arrangements in the existing tree and shade program [86]. The overall efforts will help improve the urban thermal environment and mitigate UHI effects under hot dry desert climates [87].

5. Conclusions

Urban green infrastructure provides the potential to mitigate urban heat and improve human thermal comfort in the urban residential environment. In a desert city, the scarceness of water limits the number of trees to be planted in a residential neighbourhood. Hence, it is important to understand the benefits of trees and maximize the cooling benefits of tree shade to the building structures. This paper utilizes an outdoor urban physical scale model to measure the cooling effect of tree shade with different combinations of tree densities, locations, and arrangements in a simulated compact residential neighbourhood in Tempe, AZ. The research findings quantify the tree shade cooling benefits, and indicate the effectiveness of locating shade trees in the central and east of the building's south front yard. A single full size tree can substantially cool one side of the facade hourly by up to 2.3 °C, and a cluster of two trees increase the shading benefits by up to 6.6 °C on the central part of the facade. Tree shade is also valuable to provide neighbouring shading when planting trees in the boundary of the residential parcel. This research is one of the pioneering attempts to incorporate vegetation in physical scale models to explore the shading benefits in the built environment. The research results will provide tree planting suggestions to urban planners, landscape architecture designers, and policy makers, and help the overall design and planning of urban green infrastructure in the desert city, such

as the ongoing tree and shade master plan in City of Phoenix [85] for the long-term sustainability of urban environments.

Acknowledgments: This material is based upon work supported by the National Science Foundation under grant number DEB-1637590, Central Arizona-Phoenix Long-Term Ecological Research (CAP LTER). Qunshan Zhao is partly supported by the National Natural Science Foundation of China (No. 51378399 and 41331175), the Matthew G. Bailey Scholarship Award from School of Geographical Sciences and Urban Planning, the Graduate and Professional Student Association's JumpStart Research Grant Program, and the Dissertation Research Grant from American Association of Geographers. Jiachuan Yang and Zhi-Hua Wang are supported by U.S. National Science Foundation (NSF) under grant CBET-1435881. The authors would like to thank David J. Sailor and the anonymous reviewers for their valuable comments and suggestions to improve the manuscript.

Author Contributions: Q.Z., J.Y., Z.H.W. and E.A.W. contributed to the research design. Q.Z. and J.Y. did the fieldwork experiment and data analysis. Q.Z. wrote the entire manuscript and J.Y., Z.H.W. and E.A.W. edited and improved the manuscript.

Conflicts of Interest: The authors declare no conflict of interest.

References

1. Seto, K.C.; Fragkias, M.; Güneralp, B.; Reilly, M.K. A Meta-Analysis of Global Urban Land Expansion. *PLoS ONE* **2011**, *6*, e23777. [[CrossRef](#)] [[PubMed](#)]
2. Nazaroff, W.W. Exploring the consequences of climate change for indoor air quality. *Environ. Res. Lett.* **2013**, *8*, 015022. [[CrossRef](#)]
3. Oke, T.R. The energetic basis of the urban heat island. *Q. J. R. Meteorol. Soc.* **1982**, *108*, 1–24. [[CrossRef](#)]
4. Santamouris, M. Cooling the cities—A review of reflective and green roof mitigation technologies to fight heat island and improve comfort in urban environments. *Sol. Energy* **2014**, *103*, 682–703. [[CrossRef](#)]
5. Song, J.; Wang, Z.-H. Interfacing the Urban Land–Atmosphere System through Coupled Urban Canopy and Atmospheric Models. *Bound.-Layer Meteorol.* **2014**, *154*, 427–448. [[CrossRef](#)]
6. Zhao, Q.; Myint, S.W.; Wentz, E.A.; Fan, C. Rooftop Surface Temperature Analysis in an Urban Residential Environment. *Remote Sens.* **2015**, *7*, 12135–12159. [[CrossRef](#)]
7. Zhao, Q.; Wentz, E.A. A MODIS/ASTER Airborne Simulator (MASTER) Imagery for Urban Heat Island Research. *Data* **2016**, *1*, 7. [[CrossRef](#)]
8. Tzoulas, K.; Korpela, K.; Venn, S.; Yli-Pelkonen, V.; Kaźmierczak, A.; Niemela, J.; James, P. Promoting ecosystem and human health in urban areas using Green Infrastructure: A literature review. *Landsc. Urban Plan.* **2007**, *81*, 167–178. [[CrossRef](#)]
9. Akbari, H.; Pomerantz, M.; Taha, H. Cool surfaces and shade trees to reduce energy use and improve air quality in urban areas. *Sol. Energy* **2001**, *70*, 295–310. [[CrossRef](#)]
10. Middel, A.; Chhetri, N.; Quay, R. Urban forestry and cool roofs: Assessment of heat mitigation strategies in Phoenix residential neighborhoods. *Urban For. Urban Green.* **2015**, *14*, 178–186. [[CrossRef](#)]
11. Millward, A.A.; Sabir, S. Benefits of a forested urban park: What is the value of Allan Gardens to the city of Toronto, Canada? *Landsc. Urban Plan.* **2011**, *100*, 177–188. [[CrossRef](#)]
12. Wang, Z.-H.; Zhao, X.; Yang, J.; Song, J. Cooling and energy saving potentials of shade trees and urban lawns in a desert city. *Appl. Energy* **2016**, *161*, 437–444. [[CrossRef](#)]
13. Yang, J.; Wang, Z.-H. Optimizing urban irrigation schemes for the trade-off between energy and water consumption. *Energy Build.* **2015**, *107*, 335–344. [[CrossRef](#)]
14. Yang, J.; Wang, Z.-H.; Georgescu, M.; Chen, F.; Tewari, M. Assessing the Impact of Enhanced Hydrological Processes on Urban Hydrometeorology with Application to Two Cities in Contrasting Climates. *J. Hydrometeorol.* **2016**, *17*, 1031–1047. [[CrossRef](#)]
15. Bolund, P.; Hunhammar, S. Ecosystem services in urban areas. *Ecol. Econ.* **1999**, *29*, 293–301. [[CrossRef](#)]
16. Roy, S.; Byrne, J.; Pickering, C. A systematic quantitative review of urban tree benefits, costs, and assessment methods across cities in different climatic zones. *Urban For. Urban Green.* **2012**, *11*, 351–363. [[CrossRef](#)]
17. Mullaney, J.; Lucke, T.; Trueman, S.J. A review of benefits and challenges in growing street trees in paved urban environments. *Landsc. Urban Plan.* **2015**, *134*, 157–166. [[CrossRef](#)]
18. Erell, E.; Pearlmutter, D.; Williamson, T.J. *Urban Microclimate: Designing the Spaces between Buildings*, 1st ed.; Earthscan: London, UK; Washington, DC, USA, 2011; ISBN 978-1-84407-467-9.

19. Wentz, E.A.; Rode, S.; Li, X.; Tellman, E.M.; Turner, B.L. Impact of Homeowner Association (HOA) landscaping guidelines on residential water use. *Water Resour. Res.* **2016**. [[CrossRef](#)]
20. Zhao, Q.; Wentz, E.A.; Murray, A.T. Shade Optimization in a Desert Environment. *Ext. Abstr. Proc. GISci.* **2014**, *2014*, 118–121.
21. Zhao, Q.; Wentz, E.A.; Murray, A.T. Tree shade coverage optimization in an urban residential environment. *Build. Environ.* **2017**, *115*, 269–280. [[CrossRef](#)]
22. Zhao, Q. Evaluating the Effectiveness of Tree Locations and Arrangements for Improving Urban Thermal Environment. Ph.D. Thesis, Arizona State University, Tempe, Arizona, 2017.
23. McPherson, E.G.; Simpson, J.R.; Livingston, M. Effects of three landscape treatments on residential energy and water use in Tucson, Arizona. *Energy Build.* **1989**, *13*, 127–138. [[CrossRef](#)]
24. Middel, A.; Selover, N.; Hagen, B.; Chhetri, N. Impact of shade on outdoor thermal comfort—A seasonal field study in Tempe, Arizona. *Int. J. Biometeorol.* **2016**. [[CrossRef](#)] [[PubMed](#)]
25. Song, J.; Wang, Z.-H. Impacts of mesic and xeric urban vegetation on outdoor thermal comfort and microclimate in Phoenix, AZ. *Build. Environ.* **2015**, *94*, 558–568. [[CrossRef](#)]
26. Berry, R.; Livesley, S.J.; Aye, L. Tree canopy shade impacts on solar irradiance received by building walls and their surface temperature. *Build. Environ.* **2013**, *69*, 91–100. [[CrossRef](#)]
27. Aguiar, A.C. Urban Heat Islands: Differentiating between the Benefits and Draw. Mater's Thesis, University of Wollongong, Wollongong, Australia, 2012.
28. Vanos, J.K.; Middel, A.; McKercher, G.R.; Kuras, E.R.; Ruddell, B.L. Hot playgrounds and children's health: A multiscale analysis of surface temperatures in Arizona, USA. *Landsc. Urban Plan.* **2016**, *146*, 29–42. [[CrossRef](#)]
29. Krayenhoff, E.S.; Christen, A.; Martilli, A.; Oke, T.R. A Multi-layer Radiation Model for Urban Neighbourhoods with Trees. *Bound.-Layer Meteorol.* **2014**, *151*, 139–178. [[CrossRef](#)]
30. Wang, Z.H. Monte Carlo simulations of radiative heat exchange in a street canyon with trees. *Sol. Energy* **2014**, *110*, 704–713. [[CrossRef](#)]
31. Fahmy, M.; Sharples, S. On the development of an urban passive thermal comfort system in Cairo, Egypt. *Build. Environ.* **2009**, *44*, 1907–1916. [[CrossRef](#)]
32. Stathopoulos, T.; Chiovitti, D.; Dodaro, L. Wind shielding effects of trees on low buildings. *Build. Environ.* **1994**, *29*, 141–150. [[CrossRef](#)]
33. Robitu, M.; Musy, M.; Inard, C.; Groleau, D. Modeling the influence of vegetation and water pond on urban microclimate. *Sol. Energy* **2006**, *80*, 435–447. [[CrossRef](#)]
34. Skelhorn, C.; Lindley, S.; Levermore, G. The impact of vegetation types on air and surface temperatures in a temperate city: A fine scale assessment in Manchester, UK. *Landsc. Urban Plan.* **2014**, *121*, 129–140. [[CrossRef](#)]
35. Taleghani, M.; Sailor, D.J.; Tenpierik, M.; van den Dobbelen, A. Thermal assessment of heat mitigation strategies: The case of Portland State University, Oregon, USA. *Build. Environ.* **2014**, *73*, 138–150. [[CrossRef](#)]
36. Roberts, S.M. Three-Dimensional Radiation Flux Source Areas in Urban Areas. Ph.D. Thesis, University of British Columbia, Vancouver, BC, Canada, 2010.
37. Imam Syafii, N.; Ichinose, M.; Kumakura, E.; Jusuf, S.K.; Chigusa, K.; Wong, N.H. Thermal environment assessment around bodies of water in urban canyons: A scale model study. *Sustain. Cities Soc.* **2017**, *34*, 79–89. [[CrossRef](#)]
38. Kanda, M. Progress in the scale modeling of urban climate: Review. *Theor. Appl. Climatol.* **2005**, *84*, 23–33. [[CrossRef](#)]
39. Kanda, M.; Kanega, M.; Kawai, T.; Moriwaki, R.; Sugawara, H. Roughness Lengths for Momentum and Heat Derived from Outdoor Urban Scale Models. *J. Appl. Meteorol. Climatol.* **2007**, *46*, 1067–1079. [[CrossRef](#)]
40. Kanda, M.; Kawai, T.; Moriwaki, R.; Narita, K.; Hagishima, A.; Sugawara, H. Comprehensive outdoor scale model experiments for urban climate (COSMO). In Proceedings of the 6th International Conference on Urban Climate, Göteborg, Sweden, 12–16 June 2006; pp. 270–273.
41. Kanda, M.; Moriizumi, T. Momentum and Heat Transfer over Urban-like Surfaces. *Bound.-Layer Meteorol.* **2009**, *131*, 385–401. [[CrossRef](#)]
42. Kawai, T.; Kanda, M. Urban Energy Balance Obtained from the Comprehensive Outdoor Scale Model Experiment. Part I: Basic Features of the Surface Energy Balance. *J. Appl. Meteorol. Climatol.* **2010**, *49*, 1341–1359. [[CrossRef](#)]

43. Kawai, T.; Kanda, M. Urban Energy Balance Obtained from the Comprehensive Outdoor Scale Model Experiment. Part II: Comparisons with Field Data Using an Improved Energy Partition. *J. Appl. Meteorol. Climatol.* **2010**, *49*, 1360–1376. [CrossRef]
44. Nottrott, A.; Onomura, S.; Inagaki, A.; Kanda, M.; Kleissl, J. Convective heat transfer on leeward building walls in an urban environment: Measurements in an outdoor scale model. *Int. J. Heat Mass Transf.* **2011**, *54*, 3128–3138. [CrossRef]
45. Pearlmutter, D.; Krüger, E.L.; Berliner, P. The role of evaporation in the energy balance of an open-air scaled urban surface. *Int. J. Climatol.* **2009**, *29*, 911–920. [CrossRef]
46. Pearlmutter, D.; Berliner, P.; Shaviv, E. Integrated modeling of pedestrian energy exchange and thermal comfort in urban street canyons. *Build. Environ.* **2007**, *42*, 2396–2409. [CrossRef]
47. Pearlmutter, D.; Berliner, P.; Shaviv, E. Physical modeling of pedestrian energy exchange within the urban canopy. *Build. Environ.* **2006**, *41*, 783–795. [CrossRef]
48. Pearlmutter, D.; Berliner, P.; Shaviv, E. Evaluation of Urban Surface Energy Fluxes Using an Open-Air Scale Model. *J. Appl. Meteorol.* **2005**, *44*, 532–545. [CrossRef]
49. Lirola, J.M.; Castañeda, E.; Lauret, B.; Khayet, M. A review on experimental research using scale models for buildings: Application and methodologies. *Energy Build.* **2017**, *142*, 72–110. [CrossRef]
50. Wang, Y.; Bakker, F.; de Groot, R.; Wortche, H.; Leemans, R. Effects of urban trees on local outdoor microclimate: synthesizing field measurements by numerical modelling. *Urban Ecosyst.* **2015**, *18*, 1305–1331. [CrossRef]
51. Park, M.; Hagishima, A.; Tanimoto, J.; Narita, K. Effect of urban vegetation on outdoor thermal environment: Field measurement at a scale model site. *Build. Environ.* **2012**, *56*, 38–46. [CrossRef]
52. Taleghani, M.; Tenpierik, M.; van den Dobbelen, A.; Sailor, D.J. Heat mitigation strategies in winter and summer: Field measurements in temperate climates. *Build. Environ.* **2014**, *81*, 309–319. [CrossRef]
53. Upreti, R.; Wang, Z.-H.; Yang, J. Radiative shading effect of urban trees on cooling the regional built environment. *Urban For. Urban Green.* **2017**, *26*, 18–24. [CrossRef]
54. US Census Bureau. Demographic Profile Data. 2010. Available online: <https://factfinder.census.gov/faces/tableservices/jsf/pages/productview.xhtml?src=CF> (accessed on 15 September 2016).
55. Western Regional Climate Center (WRCC). Available online: <https://wrcc.dri.edu/cgi-bin/cliMAIN.pl?az8499> (accessed on 9 July 2017).
56. Daily Summaries Station Details: PHOENIX SKY HARBOR INTERNATIONAL AIRPORT, AZ US, GHCND:USW00023183 | Climate Data Online (CDO) | National Climatic Data Center (NCDC). Available online: <https://www.ncdc.noaa.gov/cdo-web/datasets/GHCND/stations/GHCND:USW00023183/detail> (accessed on 2 January 2017).
57. Casa Grande Arizona. Available online: <https://wrcc.dri.edu/cgi-bin/rawMAIN.pl?azACSG> (accessed on 17 December 2017).
58. Maricopa County Assessor's Office. Available online: <https://mcaassessor.maricopa.gov/index.php> (accessed on 11 September 2017).
59. Shashua-Bar, L.; Pearlmutter, D.; Erell, E. The influence of trees and grass on outdoor thermal comfort in a hot-arid environment. *Int. J. Climatol.* **2011**, *31*, 1498–1506. [CrossRef]
60. Jang, H.S.; Kim, H.J.; Jeon, J.Y. Scale-model method for measuring noise reduction in residential buildings by vegetation. *Build. Environ.* **2015**, *86*, 81–88. [CrossRef]
61. Peterson, T.C.; Schmidt, R.A. Outdoor scale modeling of shrub barriers in drifting snow. *Agric. For. Meteorol.* **1984**, *31*, 167–181. [CrossRef]
62. DS1921G Thermochron iButton Device-Maxim. Available online: <https://www.maximintegrated.com/en/products/digital/data-loggers/DS1921G.html> (accessed on 15 December 2017).
63. P-Series | FLIR Systems. Available online: <http://www.flir.com/instruments/display/?id=60087> (accessed on 15 December 2017).
64. Taha, H.; Sailor, D.; Akbari, H. *High-Albedo Materials for Reducing Building Cooling Energy Use*; Lawrence Berkeley National Laboratory: Berkeley, CA, USA, 1992.
65. NOAA National Weather Service: Weather Conditions for KPHX. Available online: <http://www.wrh.noaa.gov/mesowest/timeseries.php?sid=KPHX&num=168> (accessed on 17 July 2017).
66. Papadakis, G.; Tsamis, P.; Kyritsis, S. An experimental investigation of the effect of shading with plants for solar control of buildings. *Energy Build.* **2001**, *33*, 831–836. [CrossRef]

67. Jim, C.Y. Intense summer heat fluxes in artificial turf harm people and environment. *Landsc. Urban Plan.* **2017**, *157*, 561–576. [CrossRef]
68. Jim, C.Y. Solar–terrestrial radiant-energy regimes and temperature anomalies of natural and artificial turfs. *Appl. Energy* **2016**, *173*, 520–534. [CrossRef]
69. Serensits, T.J.; McNitt, A.S.; Petrunak, D.M. Human health issues on synthetic turf in the USA. *Proc. Inst. Mech. Eng. Part P J. Sports Eng. Technol.* **2011**, *225*, 139–146. [CrossRef]
70. Villacañas, V.; Sánchez-Sánchez, J.; García-Unanue, J.; López, J.; Gallardo, L. The influence of various types of artificial turfs on football fields and their effects on the thermal profile of surfaces. *Proc. Inst. Mech. Eng. Part P J. Sports Eng. Technol.* **2017**, *231*, 21–32. [CrossRef]
71. Brabyn, L.; Zawar-Reza, P.; Stichbury, G.; Cary, C.; Storey, B.; Laughlin, D.C.; Katurji, M. Accuracy assessment of land surface temperature retrievals from Landsat 7 ETM+ in the Dry Valleys of Antarctica using iButton temperature loggers and weather station data. *Environ. Monit. Assess.* **2014**, *186*, 2619–2628. [CrossRef] [PubMed]
72. Schmid, M.-O.; Gubler, S.; Fiddes, J.; Gruber, S. Inferring snowpack ripening and melt-out from distributed measurements of near-surface ground temperatures. *Cryosphere* **2012**, *6*, 1127–1139. [CrossRef]
73. Sohrabinia, M.; Rack, W.; Zawar-Reza, P. Analysis of MODIS LST Compared with WRF Model and in situ Data over the Waimakariri River Basin, Canterbury, New Zealand. *Remote Sens.* **2012**, *4*, 3501–3527. [CrossRef]
74. Sternberg, T.; Viles, H.; Cathersides, A. Evaluating the role of ivy (*Hedera helix*) in moderating wall surface microclimates and contributing to the bioprotection of historic buildings. *Build. Environ.* **2011**, *46*, 293–297. [CrossRef]
75. Lechner, N. Sustainable Cities Are Solar-Responsive Cities. 2014. Available online: https://books.google.co.uk/books?hl=en&lr=&id=jDqDBAAAQBAJ&oi=fnd&pg=PA97&dq=Sustainable+cities+are+solar-responsive+cities&ots=SKOoY1A2we&sig=aErpxQA4Pno_cdqzZrvzyYZUxbU#v=onepage&q=Sustainable%20cities%20are%20solar-responsive%20cities&f=false (accessed on 8 January 2018).
76. Lin, Y.-H.; Tsai, K.-T. Screening of Tree Species for Improving Outdoor Human Thermal Comfort in a Taiwanese City. *Sustainability* **2017**, *9*, 340. [CrossRef]
77. Sanusi, R.; Johnstone, D.; May, P.; Livesley, S.J. Microclimate benefits that different street tree species provide to sidewalk pedestrians relate to differences in Plant Area Index. *Landsc. Urban Plan.* **2017**, *157*, 502–511. [CrossRef]
78. Middel, A.; Häb, K.; Brazel, A.J.; Martin, C.A.; Guhathakurta, S. Impact of urban form and design on mid-afternoon microclimate in Phoenix Local Climate Zones. *Landsc. Urban Plan.* **2014**, *122*, 16–28. [CrossRef]
79. Rafiee, A.; Dias, E.; Koomen, E. Local impact of tree volume on nocturnal urban heat island: A case study in Amsterdam. *Urban For. Urban Green.* **2016**, *16*, 50–61. [CrossRef]
80. Jim, C.Y. Sustainable urban greening strategies for compact cities in developing and developed economies. *Urban Ecosyst.* **2013**, *16*, 741–761. [CrossRef]
81. Brown, R.D.; Vanos, J.; Kenny, N.; Lenzholzer, S. Designing urban parks that ameliorate the effects of climate change. *Landsc. Urban Plan.* **2015**, *138*, 118–131. [CrossRef]
82. Klemm, W.; van Hove, B.; Lenzholzer, S.; Kramer, H. Towards guidelines for designing parks of the future. *Urban For. Urban Green.* **2017**, *21*, 134–145. [CrossRef]
83. Olgyay, V. *Design with Climate: Bioclimatic Approach to Architectural Regionalism*; Princeton University Press: Princeton, NJ, USA, 2015; ISBN 978-1-4008-7368-5.
84. de Abreu-Harbich, L.V.; Labaki, L.C.; Matzarakis, A. Effect of tree planting design and tree species on human thermal comfort in the tropics. *Landsc. Urban Plan.* **2015**, *138*, 99–109. [CrossRef]
85. Tree and Shade Master Plan. Available online: <https://www.phoenix.gov:443/parks/parks/urban-forest/tree-and-shade> (accessed on 17 December 2017).
86. Plant Savings with Free Shade Trees. Available online: <http://www.savewithsrp.com/RD/shadetrees.aspx> (accessed on 9 June 2016).
87. Camacho-Cervantes, M.; Schondube, J.E.; Castillo, A.; MacGregor-Fors, I. How do people perceive urban trees? Assessing likes and dislikes in relation to the trees of a city. *Urban Ecosyst.* **2014**, *17*, 761–773. [CrossRef]

